sustainability

MDPI

Article

Durability Enhancement of Sustainable Concrete Composites Comprising Waste Metalized Film Food Packaging Fibers and Palm Oil Fuel Ash

Rayed Alyousef [1,*], Hossein Mohammadhosseini [2], Ahmed Abdel Khalek Ebid [3], Hisham Alabduljabbar [1], Shek Poi Ngian [2] and Abdeliazim Mustafa Mohamed [1]

[1] Department of Civil Engineering, College of Engineering, Prince Sattam bin Abdulaziz University, Al-Kharj 11942, Saudi Arabia; h.alabduljabbar@psau.edu.sa (H.A.); a.bilal@psau.edu.sa (A.M.M.)
[2] Faculty of Engineering, School of Civil Engineering, Universiti Teknologi Malaysia (UTM), Skudai 81310, Malaysia; mhossein@utm.my (H.M.); shekpoingian@utm.my (S.P.N.)
[3] Structural Engineering and Construction Management, Faculty of Engineering, Future University in Egypt, New Cairo 11835, Egypt; ahmed.abdelkhaleq@fue.edu.eg
* Correspondence: r.alyousef@psau.edu.sa

Abstract: The utilization of waste materials in sustainable and green concrete manufacturing is particularly appealing because of the low cost of waste resources, the saving of landfill space, and the development and enhancement of concrete qualities. This paper investigates the strength and durability of green concrete composites made of waste metalized film food packaging (MFP) fibers and palm oil fuel ash (POFA). Compressive and tensile strengths, carbonation, drying shrinkage, electrical resistivity, and rapid chloride penetration tests in concrete mixtures are among the properties explored. With ordinary Portland cement (OPC), MFP fibers of 20 mm in length and six-volume fractions ranging from 0 to 1.25% were employed. Another six concrete mixes were made with 20% POFA in place of OPC. The results showed that adding MFP fibers to concrete mixes reduced their compressive strength. Despite a minor reduction in compressive strength, the inclusion of MFP fibers significantly increased tensile strength. The findings show that the combination of MFP fibers with POFA substantially impacts concrete durability. The addition of MFP fibers to concrete mixes resulted in a reduction in carbonation and drying shrinkage. The chloride penetration of specimens was also reduced, whereas the electrical resistivity of reinforced samples rose by nearly 80% compared to ordinary concrete.

Keywords: sustainable concrete composites; waste metalized polypropylene fibers; strength properties; rapid chloride penetration; electrical resistivity

Citation: Alyousef, R.; Mohammadhosseini, H.; Ebid, A.A.K.; Alabduljabbar, H.; Ngian, S.P.; Mohamed, A.M. Durability Enhancement of Sustainable Concrete Composites Comprising Waste Metalized Film Food Packaging Fibers and Palm Oil Fuel Ash. *Sustainability* **2022**, *14*, 5253. https://doi.org/10.3390/su14095253

Academic Editors: Quoc Tri Phung and Nguyen Van Tuan

Received: 20 March 2022
Accepted: 25 April 2022
Published: 26 April 2022

1. Introduction

The primary aim of developing cleaner production is to reduce industrial waste and natural resource usage. Cleaner production refers to procedures that improve production quality by improving eco-efficiency and using fewer raw resources. The number and varieties of solid waste materials have expanded with population growth, industrialization, and urbanization. Several forms of non-biodegradable waste materials will last hundreds, if not thousands, of years in the environment. Non-biodegradable waste products negatively impact trash disposal and constitute a severe environmental hazard. To maintain the long-term viability of green building, increased emphasis is being placed on efficient and effective waste management. As a result, waste material used is one of the most important aspects of waste management plans in many regions of the world [1–3].

Waste minimization has an excellent promise for cleaner manufacturing since it improves energy efficiency, reduces energy use, and enhances an industry's technical functioning. The concept of sustainability advocates using waste products to substitute raw

resources such as fine and coarse aggregates, cement, and fibrous materials in the building sector. This would lead to environmentally friendly and sustainable buildings by lowering the cost of the materials due to the replacement and the expenses of adequately managing waste materials [4]. Low energy costs are associated with green materials, and their use must be long-lasting and low-maintenance, resulting in durable construction materials [5,6].

By 2015, global plastic usage had reached 297.5 million tons, with Asia accounting for 30% of global consumption during the previous few years. Plastic garbage accounts for around 16% of the total municipal solid waste weight. Polyolefin, a popular plastic, is less biodegradable, and when disposed of as solid trash, it has a long-term detrimental impact on the environment. The biodegradation of various types of plastics in natural soils, such as high-density polyethylene (HDPE), low-density polyethylene (LDPE), polypropylene (PP), and polystyrene (PS), revealed that some soil microorganisms, such as fungi and bacteria, have a specific metabolic capacity to assimilate these plastics as carbon and energy sources for their growth [7]. About half of these materials were single-use consumer products, which had a considerable impact on the increase in plastic waste. According to Sharma and Bansal [8], plastics contribute an ever-increasing volume to the solid waste stream because of their wide variety of applications. As a result, quantitative data on plastic waste output is rarely made public because it is generally kept in-house or managed commercially. According to Plastics Europe, Europe creates 25 million tonnes of plastic trash each year [9]. More than a quarter of the waste generated in the United States in 2014 was efficiently repurposed, while the rest went to energy recycling and landfills [10].

Global recycling and energy recovery rates have gradually increased over the past decade, resulting in decreased landfilling. The rate of landfilling varies substantially across Europe. Landfill bans have resulted in fewer than 10% of plastic waste disposal. Nearly half of all plastic waste winds up in landfills in other countries, according to Eriksen et al. [11]. According to Faraca and Astrup [12], most plastics are non-biodegradable and chemically inert in nature. This type of polymer-based product has the potential to last decades or perhaps centuries in the environment. As a result of chemical reactions in certain plastics, such as PC, PP, and PVC, hazardous compounds may be released into the air, water, and soil [13]. Consequently, discarded plastics in any form are considered a big environmental concern in the eyes of the public.

Nonetheless, though not all types of waste polymers, most plastic wastes may be reused and treated thermally or chemically [14]. Waste metalized polypropylene (MFP) films are produced and dumped in landfills worldwide. They are primarily used in food packaging and are made of polymeric materials with a thin aluminum coating on top. MFP is the least processable and recyclable of all plastic wastes [9]. Because there is no suitable way to recycle such a large quantity of waste plastics, they are disposed of in landfills and burned [15,16]. As a result, reliable disposal methods to replace existing methods have become necessary.

Concrete is a well-known building material worldwide owing to the accessibility of materials, simplicity of manufacture, and good durability and mechanical properties [17]. Nonetheless, due to its widespread use, particularly in the industrial sector, concrete is constantly subjected to chemical assaults. These attacks can occur naturally, such as sulfates in soils and groundwater, or through human-caused chemical attacks, such as drainage wastewater and industrial sewage, which degrade the performance of structures and limit their service life. Liu et al. [18] suggested that the degradation of concrete might be caused by chemical processes caused by ion exchange in such hostile settings. As a result of these actions, the hydration products degrade, and hazardous compounds such as ettringite and gypsum particles develop in the concrete. Consequently, the concrete microstructure produces cracks, spalling, and inequalities, reducing the strength and durability of concrete buildings [19,20]. According to Abro et al. [21] and Buller et al. [22], cracking is one of the most common difficulties with plain concrete subject to chemicals, and practical approaches are required to reduce the brittleness of concrete components under chemical attacks. They pointed out that using short fibers can strengthen concrete

and improve the performance of concrete in harsh conditions through enhancement in the brittleness of concrete. Furthermore, Alrshoudi et al. [23] and Alnahhal et al. [24] found that employing pozzolanic materials as partial cementing materials, such as palm oil fuel ash (POFA), enhanced the performance of concrete subjected to chemical assaults by lowering the rate of mass loss and strength loss.

There is no doubt that special attention is being paid to the cleaner and more efficient management of various types of waste generation to ensure sustainability in green buildings. One of the essential concerns in waste management techniques is waste products. Recycling benefits the environment by lowering pollution, minimizing landfilling and waste disposal, and protecting natural resources. A novel concrete form has been developed using waste plastics as fibrous components and POFA as a partial cement substitute. Because POFA is a pozzolanic material, it was employed to create concrete composites and the local availability of waste plastics. Given the argument mentioned above, the goal of this study was to look into the combined impacts of waste plastic fibers and POFA on concrete performance and see how plastic fibers contribute to better energy absorption when compared to plain concrete without any fibers. The use of discarded plastic fibers and POFA in green and sustainable concrete manufacturing might have environmental and economic benefits.

Furthermore, it is useful since it reduces landfilling issues and the consumption of raw materials while increasing the creation of green and sustainable construction materials. As a result of the current literature, it has been suggested that pozzolanic materials and short fibers improve the performance of concrete subjected to chemical assaults. The objective of this study was to investigate the combined effects of waste plastics and POFA on the strength and durability performance of concrete. Although this research includes an investigation of polymeric-based fibers, such as polypropylene (PP), the conducted experiments and analyses are based on one type of fiber: waste metalized film food packaging (MFP). The work has focused on the performance of concrete containing MFP fibers and POFA exposed to chemicals, but rather it is believed that technical issues have to be understood and fixed right before utilizing any waste fibers in concrete. In this study, a comparison was made between the electrical resistivity, rapid chloride penetration, drying shrinkage, and the strength of both concrete mixtures containing MFP fibers and plain concrete. Moreover, X-ray diffraction (XRD) and scanning electron microscopy (SEM) were carried out to investigate the microstructure of concrete composites.

2. Experimental Program

2.1. Materials

A type I cement that met the ASTM C 150-07 requirements was employed in this investigation. Furthermore, POFA was replaced with OPC at a 20% substitution level. The waste from the local mill sector was used to gather the raw palm oil fuel ash particles. The ash particles were dried at 100 °C before sieving to eliminate the bigger particles larger than 150 μm. The tiny ash particles were then stored in a crushing machine, and the grinding operation was repeated for around two hours for every 4 kg of ash. The grounded POFA particles were tested according to BS 3892: 1-1992 and ASTM C618-15 requirements to acquire the requisite characteristics, as shown in Figure 1. As cementing materials, the ashes that met the required standards and had the appropriate chemical compositions and physical qualities were employed, as shown in Table 1. Natural river sand was used, with a specific gravity of 2.6 g/cm^3, a fineness modulus of 2.3, water absorption of 0.7%, and a maximum size of 4.75 mm. Crushed granite coarse aggregates with water absorption of 0.5%, a specific gravity of 2.7 g/cm^3, and a maximum size of 10 mm were employed. Waste metalized film food packaging fibers with an aluminum metalization procedure used in food packaging were collected as trash and cleaned to remove any contaminants. The waste films were then split into 2 mm wide and 25 mm long fibers, as illustrated in Figure 2. Table 2 shows the typical engineering parameters of MFP fiber employed in this work.

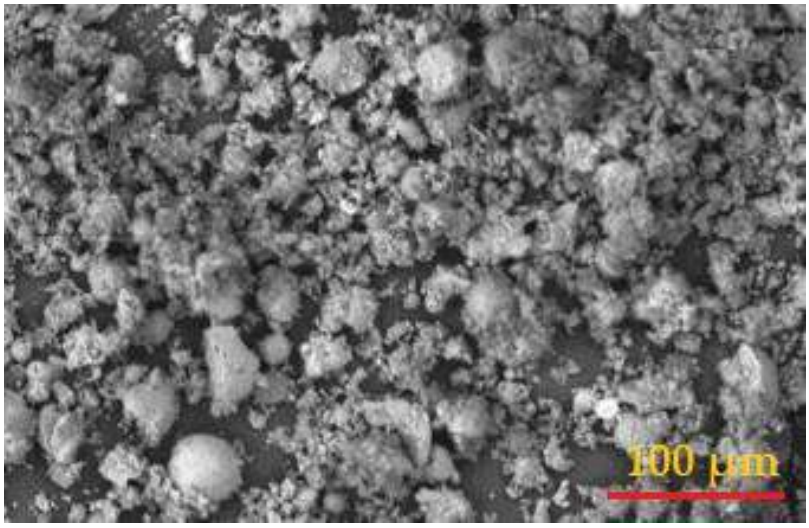

Figure 1. SEM image of POFA particles.

Table 1. Properties of OPC and POFA.

Material	Physical Properties		Chemical Composition (%)							
	Specific Gravity	Blaine Fineness	SiO_2	Al_2O_3	Fe_2O_3	CaO	MgO	K_2O	SO_3	LOI
OPC	3.15	3990	20.3	5.3	4.21	62.5	1.53	0.005	2.13	2.35
POFA	2.42	4930	62.7	4.8	8.14	5.8	3.54	9.07	1.17	6.28

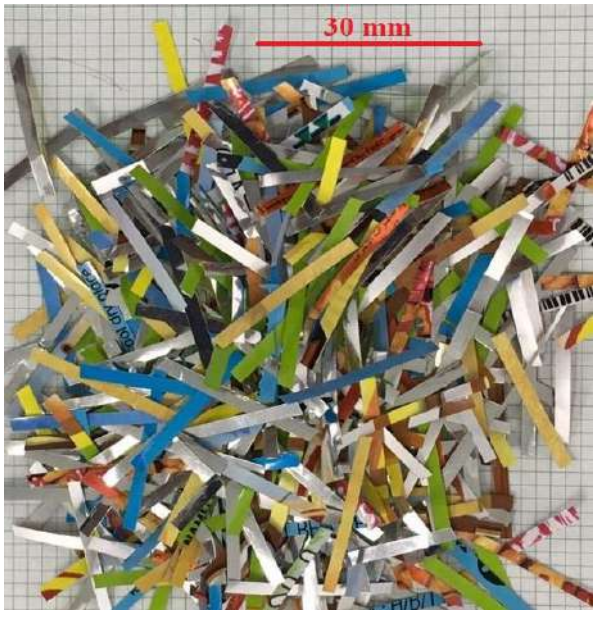

Figure 2. The fabricated waste metalized film food packaging fibers.

Table 2. Typical properties of MFP fibers.

Type of Resin	Size (W × L) (mm)	Density Range (kg/m^3)	Thickness (mm)	Tensile Strength (MPa)	Elongation (%)
Polypropylene	2 × 25	0.94	0.08	560	8–10

2.2. Mix Proportions and Testing Methods

Table 3 shows the mixed proportions of various components utilized in producing concrete composites. In total, 12 concrete mixes were made, of which the first batch was the control mix without any POFA and fibers. Among the twelve mixes, six batches contained OPC with fiber volume fractions of 0%, 0.25%, 0.5%, 0.75%, 1.0%, and 1.25% (B1–B6). Another six batches were made with POFA replacing OPC by 20% for the same fiber volume fractions (B7–B12) with a constant water/binder (w/b) ratio of 0.48. The procedure of combining components for fiber-reinforced concrete differs slightly from that of conventional cement. POFA and OPC were added to a dry mix of fine and coarse aggregates in the first phase. The superplasticizer and water were added and stirred for about two minutes. Finally, the desired amount of fibers was added to the mixture, and the mixing process was maintained for another two minutes to ensure that the fibers were uniformly distributed throughout the mixture.

Table 3. The details of mix proportions for various concrete mixtures.

Mix	Cement (kg/m^3)	POFA (kg/m^3)	Water (kg/m^3)	Fine Aggregate (kg/m^3)	Coarse Aggregate (kg/m^3)	V_f (%)
B1	440	-	212	835	855	0.0
B2	440	-	212	835	855	0.25
B3	440	-	212	835	855	0.50
B4	440	-	212	835	855	0.75
B5	440	-	212	835	855	1.0
B6	440	-	212	835	855	1.25
B7	352	88	212	835	855	0.0
B8	352	88	212	835	855	0.25
B9	352	88	212	835	855	0.50
B10	352	88	212	835	855	0.75
B11	352	88	212	835	855	1.0
B12	352	88	212	835	855	1.25

To evaluate compressive strength, cubic samples with 100 mm sides were constructed following BS EN 12390:2-09 and BS EN 12390-3:09. Cylindrical specimens of 100 × 200 mm were prepared according to ASTM C496-11 and ASTM C512, respectively, for splitting tensile strength and drying shrinkage measurements. After curing the concrete specimens in the water tank for 28 days, a drying shrinkage test was carried out from day 1 to day 180. The samples were placed in a drying chamber with controlled temperature and humidity for the test period after the curing period was completed. Furthermore, 100 × 200 mm cylindrical specimens were exposed to a carbon dioxide (CO_2) prone atmosphere to assess the carbonation attack on concrete. The carbonation depth of concrete specimens under CO_2 diffusion might be used to determine the carbonation resistance of the concrete. The procedure proposed by RILEM Committee CPC-18 was followed throughout the test. The depth of carbonation appeared by spraying phenolphthalein solution on the split sides of concrete specimens, as revealed in Figure 3. It can be seen that the color of the un-carbonated area changed to purple, while the color of the carbonated area remained colorless. At 90 and 180 days of age, researchers measured carbonation depth. The space among the edge of the specimens and the purple color boundary was therefore used to determine the average depth of carbonation.

According to ASTM C1202-12, a rapid chloride penetration test was performed. The test was conducted on 100 × 50 mm cylindrical samples that were adequately cured and saturated on the surface after 28 and 90 days of curing. The saturated specimen was placed between two plexiglass specimen cells, and the edges of the sample and the cells were sealed with a high viscosity sealant. A 0.3 N sodium hydroxide (NaOH) solution was put into the cell linked to the power supply's positive terminal. The cell connected to the negative terminal, on the other hand, was filled with a 3% sodium chloride (NaCI) solution.

The power was supplied by an APLAB-regulated DC power supply, model 7231, with a shunt resistor for current measurement. For each curing age, three different specimens were tested. Sixty volts (60 v) DC potential difference was maintained throughout the specimen for six hours, with current readings taken every 30 min. The total charge traveled through the concrete sample was computed, and the appropriate corrections were performed using Equation (1). Moreover, the OPC and POFA concrete samples were immersed in a 5% sodium chloride (NaCl) solution for 90 days to analyze the microstructure of the samples by using scanning electron microscopy (SEM) and X-ray diffraction (XRD) under the chloride attack.

$$Q = 900(Io + 2I_{30} + 2I_{60} + \ldots\ldots + 2I_{300} + 2I_{330} + 2I_{360}) \quad (1)$$

where Q is the charge passed (coulombs) and I is the current (amperes) at a given time (t = 0 to 360 min).

Figure 3. Indication of the depth of carbonation in concrete specimens by using phenolphthalein solution.

The Resipod SFE 2011.03.31, a high-resolution Proceq brand electric resistivity meter, assessed the concrete's electrical resistivity. In line with AASHTO-TP-95-11, the test was conducted utilizing the four-point Wenner array probe technique. At 28 and 90 days, the test was performed on sufficiently cured and saturated surfaces with 100 × 200 mm cylindrical samples. Four quaternary longitudinal positions of the specimen were measured, and each location was measured once. Consequently, 24 resistivity measurements for three specimens were collected. The electrical resistivity of the concrete was calculated by averaging the measurements recorded for each sample.

3. Results and Discussion

3.1. Compressive Strength

Figure 4 shows the compressive strength test results for concrete mixtures, including MFP fibers. The outcomes revealed that adding MFP fiber to the concrete reduced the compressive strength. The results showed that at ages beyond 90 days, the acquired strength values in POFA mixes were more significant than in OPC mixes. The 28-day compressive strengths of OPC concrete mixes comprising 0.25, 0.5, 0.75, 1, and 1.25% MFP fibers were 40.1, 39.4, 37.9, 35, and 33.5 MPa, correspondingly, which are slightly lower than the 42.8 MPa noted for the plain concrete mix with 0% MFP fibers. Similarly, at 28 days, adding the same volume fractions of MFP fibers to POFA mixes resulted in compressive strengths of 35.1, 33, 30.8, 29.1, and 26.5 MPa, respectively, which are lesser

than the 38.5 MPa observed for the POFA-plain mix. It can be noticed that the acquired strength values of POFA mixtures were somewhat lesser than those of POFA mixes after a 28-day curing time. It might be due to POFA's delayed hydration rate, which causes lower strength levels at a young age. Furthermore, cavities in concrete specimens, caused by a lack of hydration products in POFA mixes, and the balling effect caused by a larger fiber dosage, result in significantly lower strength values [25].

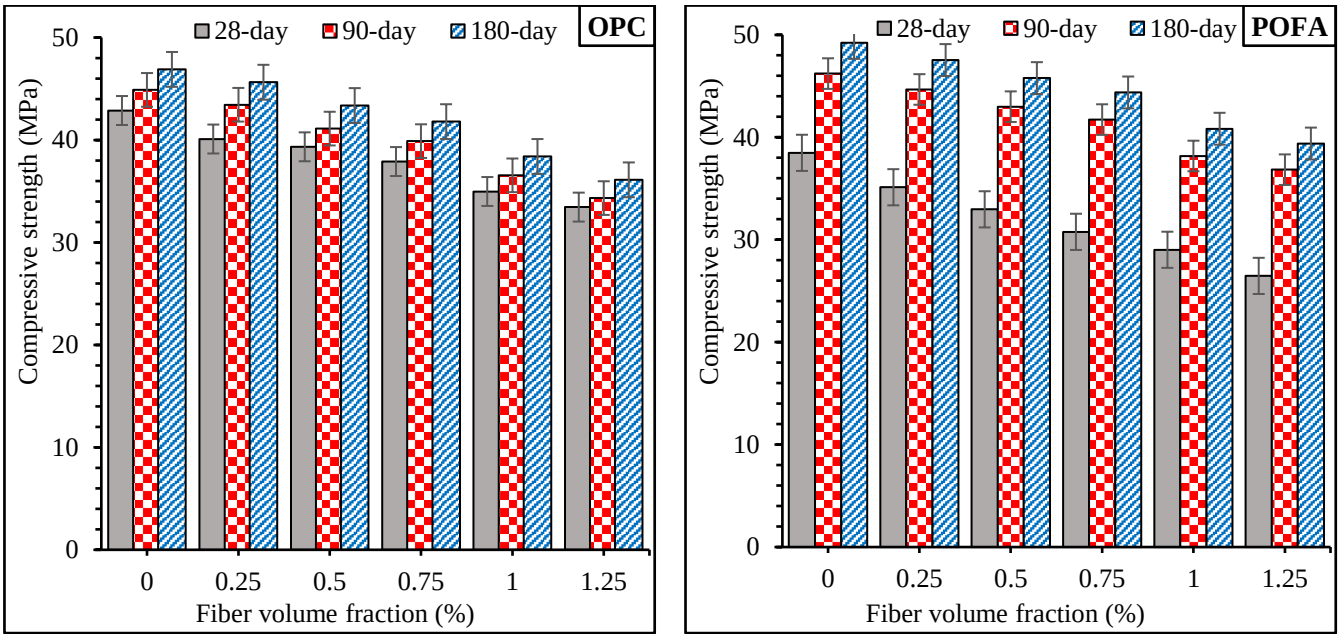

Figure 4. Compressive strength of concrete mixes comprising MFP fibers.

Nevertheless, due to the utilization of POFA and its strong pozzolanic characteristic, the obtained strengths of concrete mixes were significantly larger than those of the early age after a prolonged curing period of 180 days. For example, compressive strengths of 47.6, 45.8, 44.4, 40.8, and 39.4 MPa were observed for the POFA mixes with the same fiber content after 180 days of curing, which are all higher than 30 MPa, and based on the standard specifications, they can be used as structural application. The OPC mixes with the same fiber doses had lower compressive strength values of 45.6, 43.7, 41.8, 38.4, and 36.1 MPa. It was discovered that the POFA mixtures had better strength values than the OPC specimens while having equal fiber contents. This study's findings are comparable to those published by Mujedu et al. [26], who demonstrated a considerable increase in concrete compressive strength by employing POFA as a partial cement substitute during extended curing times.

3.2. Tensile Strength

The outcomes of the tensile strength test for concrete mixes comprising MFP fibers at different ages are shown in Figure 5. It can be observed that the addition of MFP fibers prominently improved the tensile strength of all concrete mixtures, and all reinforced concrete specimens have better tensile strength than the control mix. At 90 days and beyond, the strength development of POFA mixes was greater than that of OPC combinations. The inclusion of MFP fibers at doses of 0.25, 0.5, 0.75, 1, and 1.25% resulted in tensile strengths of 3.4, 3.61, 3.65, 3.46, and 3.3 MPa, respectively, after a 28-day curing time, which is all greater than the control mix's 2.93 MPa. For the same fiber doses, lower tensile strengths of 3.2, 3.4, 3.28, 3.18, and 2.92 MPa were reported for POFA mixes. Furthermore, the tensile strengths of POFA mixes were greater than those of OPC mixes, including MFP fibers, after a more extended curing age of 180 days. The 180-day tensile strength of POFA mixes was 4.63, 5.02, 4.82, 4.74, and 4.59 MPa for the same fiber content, which is somewhat higher than the values of 4.49, 4.76, 4.7, 4.5, and 4.26 MPa for OPC mix, respectively.

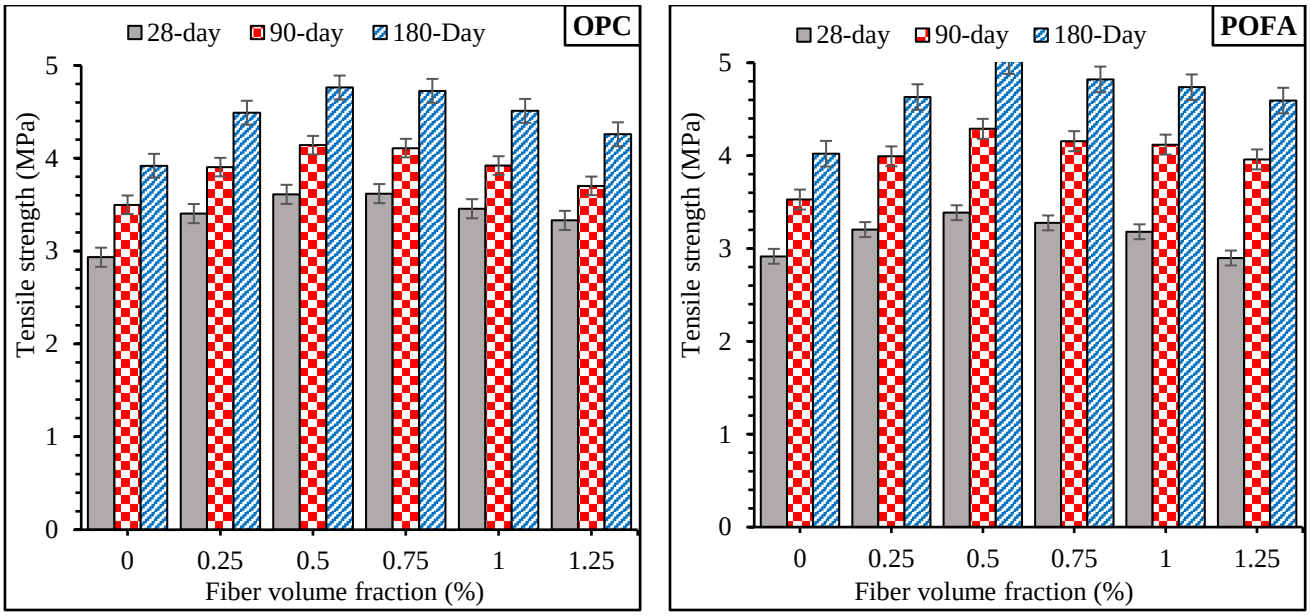

Figure 5. Tensile strength of concrete mixtures reinforced with MFP fibers.

MFP fibers were shown to have an enhanced ability to bear the splitting stress after failure without entirely collapsing in most cases. Additionally, reinforced specimens' failure modes were more ductile than plain concrete specimens. The high tensile strength of POFA mixes reinforced with MFP fibers during extended curing times might be attributable to the strong bond between MFP fibers and concrete matrix and the bridging effect of the fibers, which prevents micro-cracks and avoids specimens from collapsing suddenly. Furthermore, due to the creation of additional hydration products, POFA's pozzolanic activity resulted in better concrete strength enhancement, particularly during longer curing durations [27]. The contact area between fibers and matrix is reduced with greater doses of fibers due to plastic fibers' behavior and their limited connecting characteristics, resulting in lower tensile strength values. On the other hand, all enhanced specimens exhibited better tensile strength than ordinary mixtures [28].

3.3. Carbonation

Figure 6 shows the natural carbonation depths of concrete mixes with varied MFP contents after 90 and 180 days of outdoor exposure. When MFP fibers were introduced to the concrete composite, the carbonation depth was lowered. OPC concrete composites had lower carbonation depths than ordinary concrete for fiber dosages of 0.75%. For concrete mixes comprising 0.25, 0.5, and 0.75% fiber, carbonation depths of 0.57, 0.54, and 0.5 mm have been observed. After 180 days of exposure, these findings were lesser than the 0.66 mm achieved by the control mix. For carbonation depth to grow above 0.75%, the fiber content must be increased. A depth of 0.77 mm was found in the mix containing 1.25% fibers. An earlier study by Zhang and Li [29] found that carbonation in concrete composites was affected by the presence of PP fiber.

It is recognized that carbonation propagation is the process by which CO_2 is diffused into concrete from the surrounding environment, and as the CO_2 diffusion depth increases, the carbonation depth also increases. As well as the presence of pores and micro-cracks in the concrete itself, carbonation is brought on by external factors. To reduce capillary porosity, an ordered network of short fibers is intended to be provided by the concrete composite's homogenous dispersion of fibers. Furthermore, fibers' anti-cracking properties may reduce the number of cracks in concrete composites. As a result, the inclusion of polymeric-based fibers into concrete composites improves carbonation resistance [30,31].

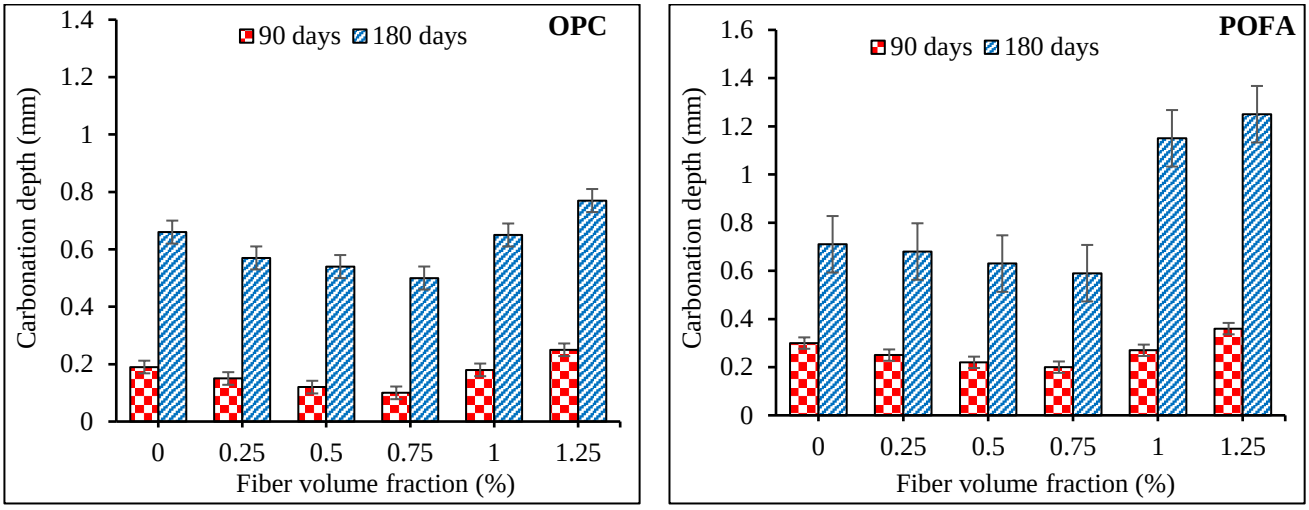

Figure 6. Variation in the carbonation depth of concrete mixtures containing MFP fibers.

The comparatively modest quantity of OPC in the concrete mix and the low pozzolanic activity of POFA particles at early ages can be attributed to the increased carbonation in the specimen containing POFA. However, because the test was done using a sample that had been preserved for 28 days in a water tank, the hydration of the POFA specimen was compromised. Accordingly, the strength growth will be hampered, and resistance to the entry of harmful chemical particles will be reduced. POFA mixes have less calcium hydroxide ($Ca(OH)_2$) than standard concrete that does not contain POFA. Since the amount of $Ca(OH)_2$ in POFA concrete is decreasing, there is an increased risk of CO_2 intrusion from the environment, which might lead to accelerated carbonation [32]. $Ca(OH)_2$ formed during OPC hydration interacts with POFA as the pozzolanic process progresses, reducing the concentration of $Ca(OH)_2$. CO_2 reacts with $Ca(OH)_2$ during the carbonation process. After the pozzolanic reaction has reacted with the calcium hydroxide in certain spots, CO_2 will penetrate deeper into the concrete specimen to react with the existing $Ca(OH)_2$, and the carbonation depth will surge. Nevertheless, satisfactory curing of POFA concrete is projected to reduce carbonation owing to the tighter pore refinement structure that results from the pozzolanic response of the POFA at longer periods [33,34].

3.4. Drying Shrinkage

The influence of MFP fibers on the drying shrinkage behavior of the concrete composite was investigated in this study. With the addition of MFP fibers to all mixtures, the drying shrinkage of the concrete was reduced. The most considerable drying shrinkage in the OPC concrete samples arose in the control plain mix, as shown in Figure 7. Compared to the OPC control combination, the mixtures comprising 0.25, 0.5, 0.75, 1, and 1.25% MFP fibers caused 10.6, 25.7, 16, and 5.5% decreases in drying shrinkage after 180 days. Furthermore, the combination with 0.75% fibers showed the least drying shrinkage. The superior tensile behavior of concrete and the connecting action of fibers along fractures were credited with reducing shrinkage for mixes, including up to 0.75% fiber. The POFA concrete mixtures were additionally reinforced with MFP fibers, as seen in Figure 6. Compared to the POFA concrete prepared without fibers, the concrete with 20% POFA incorporating the same MFP fiber content showed lower drying shrinkage of 11.5, 24, 29.9, 18.5, and 6%, respectively.

Because the test was done using specimens cured for 28 days, the hydration process of POFA specimens was delayed initially in the curing period. As a result, strength development will be impaired, and drying shrinkage will be enhanced. On the other hand, short fibers reduced shrinkage marginally by performing as a connection among the matrix and aggregates. Owing to the pozzolanic character of POFA and the generation of extra hydration product over prolonged curing times, a strong link was created between the fibers and the cement matrix, resulting in reduced drying shrinkage values. Fly ash concrete

incorporating PP fiber exhibited very minimal drying shrinkage, according to Karahan and Atis [35]. They also discovered that the increase in fiber content was associated with a decrease in drying shrinkage.

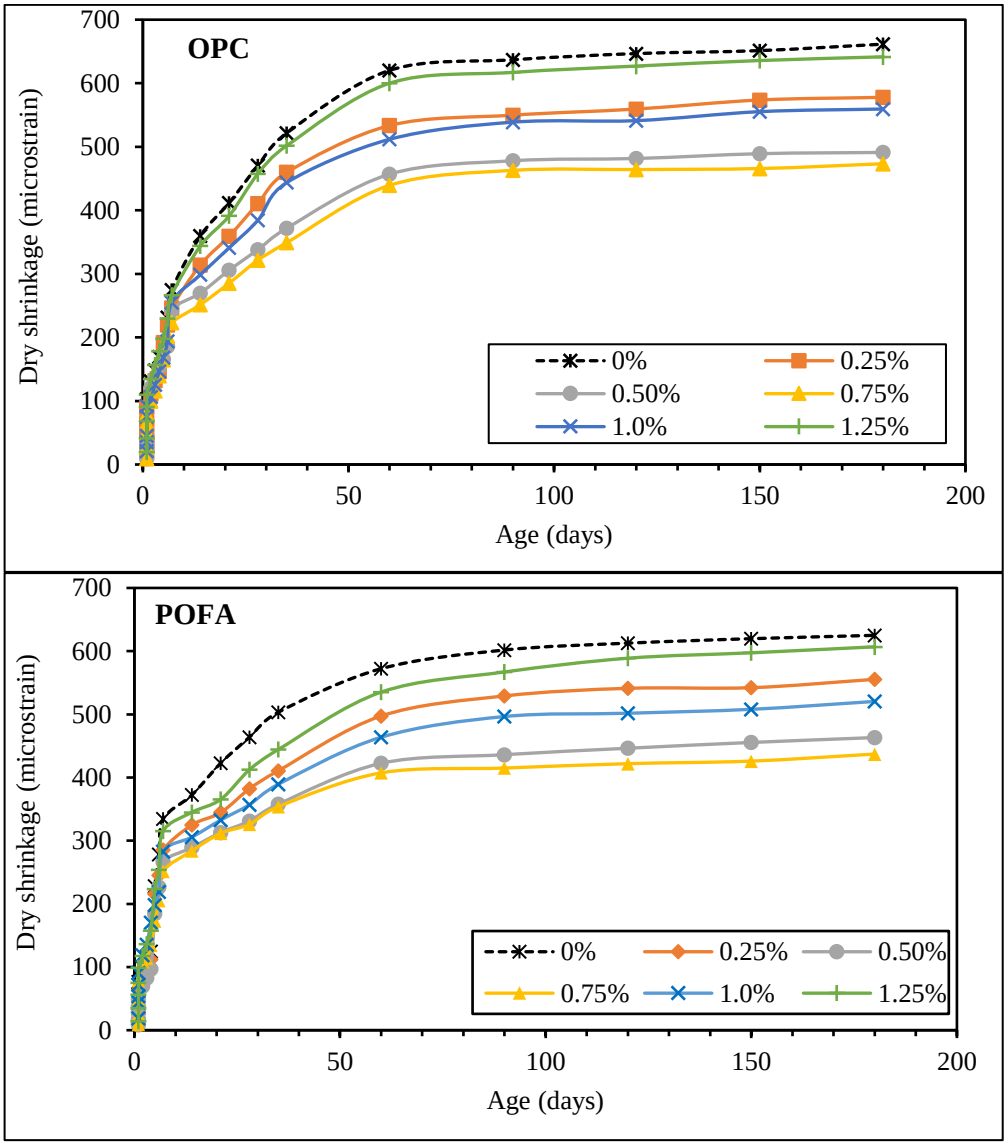

Figure 7. Variation in the drying shrinkage of concrete mixtures reinforced with MFP fibers.

3.5. Electrical Resistivity

Different tests may be used to determine the corrosion resistance of reinforcing bars in concrete. A non-destructive method of electrical resistivity test can be used for assessing the risk of corrosion based on existing classifications [36]. A greater electrical resistance signifies a decreased rate of corrosion. The average electrical resistivity test results of the various concrete mixes, including MFP fibers, are shown in Figure 8. The concrete mixes had true electrical resistivity ranging from 18.5 to 43.7 kΩ·cm. According to Wang and Aslani [37], the genuine electrical resistivity of concrete must be larger than 5 kΩ·cm because the corrosion rate is considerable below this level. When the genuine electrical resistivity of concrete is between 5 and 10 kΩ·cm, it is considered to have a moderate to low corrosion rate; however, when the true electrical resistivity is over 10 kΩ·cm, it is said to have strong corrosion resistance [38].

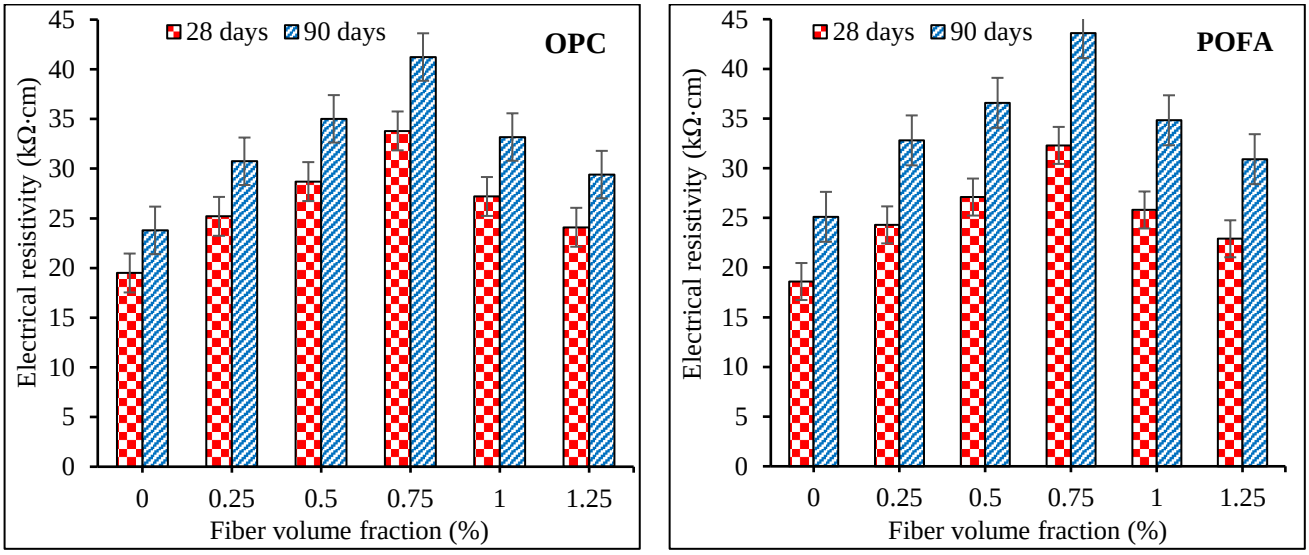

Figure 8. Electrical resistivity of concrete mixtures reinforced with MFP fibers.

All of the concrete mixes in this investigation had an electrical resistance greater than 10 kΩ·cm. At 90 days, however, the actual electrical resistivity values were greater. Electrical resistivity values of 30.7, 35.1, 41.3, 33.2, and 29.4 kΩ·cm were observed for the OPC mixes comprising 0.25, 0.5, 0.75, 1, and 1.25% MFP fiber, respectively, which are all greater than the 23.8 kΩ·cm reported for the OPC plain concrete. Similarly, the electrical resistivity values for the POFA mix reinforced with the same fiber quantities were 32.8, 36.6, 43.6, 34.8, and 30.9 kΩ·cm, respectively, and the resultant values are greater than the 25.1 kΩ·cm found for the plain mix.

The findings show that adding POFA to concrete significantly impacts its electrical resistivity. Compared to OPC mixes, substituting 20% of cement weight with POFA increased the 90-day electrical resistivity. This is owing to POFA's pozzolanic activity, which densifies the microstructure of concrete and, as a result, modifies the ion species and concentrations in the concrete matrix. Lim et al. [39] found that when mineral admixtures were added to the concrete mixture, the additional hydration products such as C-S-H and C-A-H gels filled the micro-voids in the matrix, lowering porosity and pore connectivity, subsequently increasing electrical resistance. It was discovered that the combination including both POFA and 0.75% MFP fibers had the highest electrical resistance.

3.6. Rapid Chloride Penetration

One of the most serious matters that can affect concrete structures is durability, especially as the issue of sustainability becomes increasingly vital. Durable structures survive longer than nondurable structures, ensuring the concrete structures' long-term viability. Permeability is the most critical attribute of a reinforced concrete structure's long-term performance. The distribution, size, and connectivity of micro-cracks and voids are the essential microstructural features determining concrete permeability [40,41]. The chloride penetration of concrete was employed in this study to measure permeability as it influences durability. Figure 9 shows the chloride ion penetration of various concretes with and without fibers. Figure 8 shows the rapid chloride ion penetration findings determined by the electric charge transmitted in coulombs through the reinforced MFP fibers in concrete specimens. According to the ASTM C1202-12 specifications, the chloride ion penetrability based on charges passed is considered very low for values between 100 and 1000 C, low for values between 1000 and 2000 C, moderate for values between 2000 and 4000 C, and high for values greater than 4000 C. It can be seen that the obtained values range from 230 to 290 C, which could be considered to be within the acceptable range.

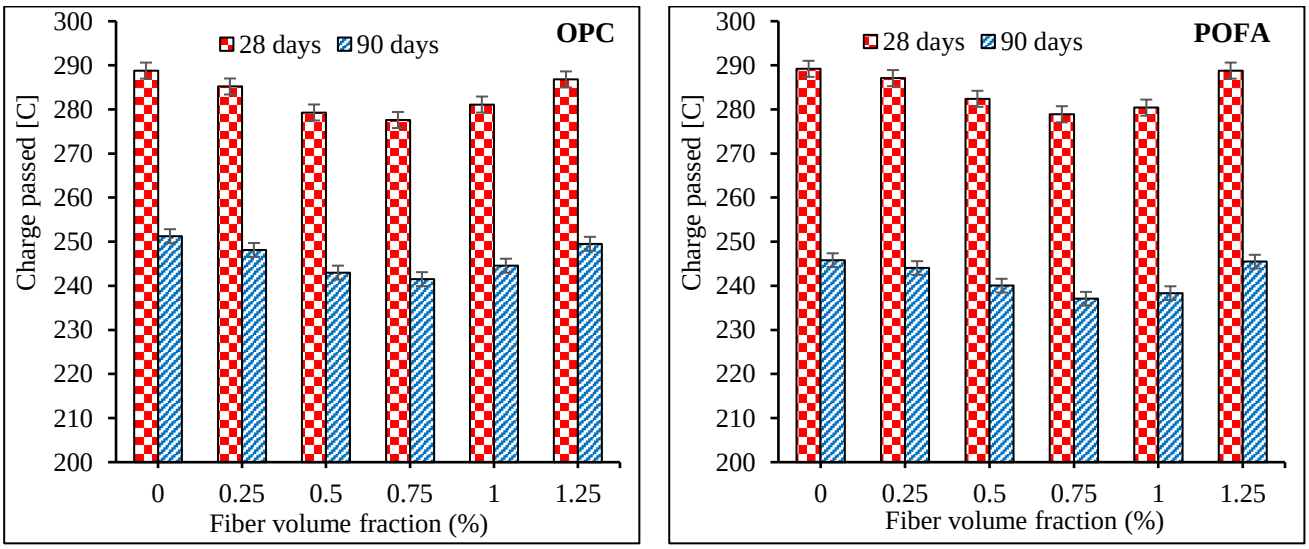

Figure 9. Rapid chloride penetration of concrete mixtures reinforced with MFP fibers.

Figure 9 further shows that adding MFP fibers to concrete mixes reduces chloride penetration. The addition of 0.25, 0.5, 0.75, 1, and 1.25% MFP fibers to OPC mixes at 90 days results in charge passed values of 248.1, 242.9, 241.5, 244.6, and 249.5 C, respectively, which are lesser than the control OPC mix's charge passed value of 251.3 C. Similarly, charge passing values of 244, 240.1, 237, 238.4, and 245.5 C were observed for the POFA mixtures reinforced with the same fiber contents that are lesser than the 245.8 C reported for the control POFA mix. In this context, Afroughsabet et al. [42] found that the inclusion of PP fibers reduced the chloride migration coefficient of FRC, but the addition of steel fibers increased it. The inclusion of conductive materials such as steel fibers considerably increases the concrete's chloride passage coefficient since the quick chloride penetration test is connected to the electric current that travels over the concrete matrix.

In addition, Figure 10 shows the relationship between electrical resistivity and rapid chloride ion penetration in concrete mixes reinforced with MFP fibers. The electrical resistivity and the rapid chloride penetration were linearly correlated with the goodness of fit (R^2) of 0.7087, which indicates the reliable nature of the data. Because the more significant the electrical resistivity, the better the concrete durability, and the lower the rapid chloride penetration, the better the concrete durability, such a good association was discovered. Consequently, a negative correlation between the two values indicates that the durability qualities are sufficient.

POFA, which had a finer particle size than OPC, produced matrix densification and filled holes with extra hydration products such as C-S-H gel, resulting in decreased chloride penetration [43]. The amount of $Ca(OH)_2$ was reduced due to the hydration process and the development of POFA's pozzolanic activity. Consequently, increased $Ca(OH)_2$ consumption led to the creation of a new C-S-H gel, which reduced void size and resulted in a more solid matrix with lower porosity and diffusion depth. SEM images of water-cured and chloride immersion OPC and POFA concrete samples are shown in Figures 11 and 12, respectively. The formation of C-S-H gel can be detected in SEM pictures of concrete mixtures cured in water, as shown in Figure 11. The microstructure of the mixtures altered regularly as the cure period continued. The C-S-H gels in the POFA-based mixture are more consistently spared than the OPC-based mixture after 90 days of water curing. Several crystallines appear to intersect with the C-S-H gel in the OPC concrete mixture. There are a few voids apparent among the crystals as well. The POFA mix, on the other hand, contains fewer holes and more gel components than OPC concrete. In the POFA mix, a network of C-S-H gels developed, resulting in a denser matrix. This is attributed to POFA's pozzolanic performance, which improved the microstructure of the concrete matrix by

producing pozzolanic activity and the formation of additional C-S-H gels over the longer curing times [44].

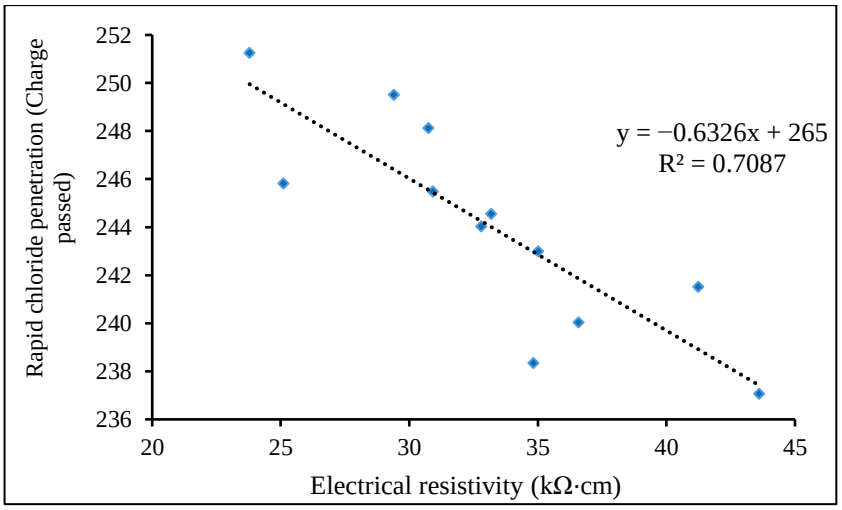

Figure 10. Correlation between electrical resistivity and rapid chloride penetration of concrete mixtures.

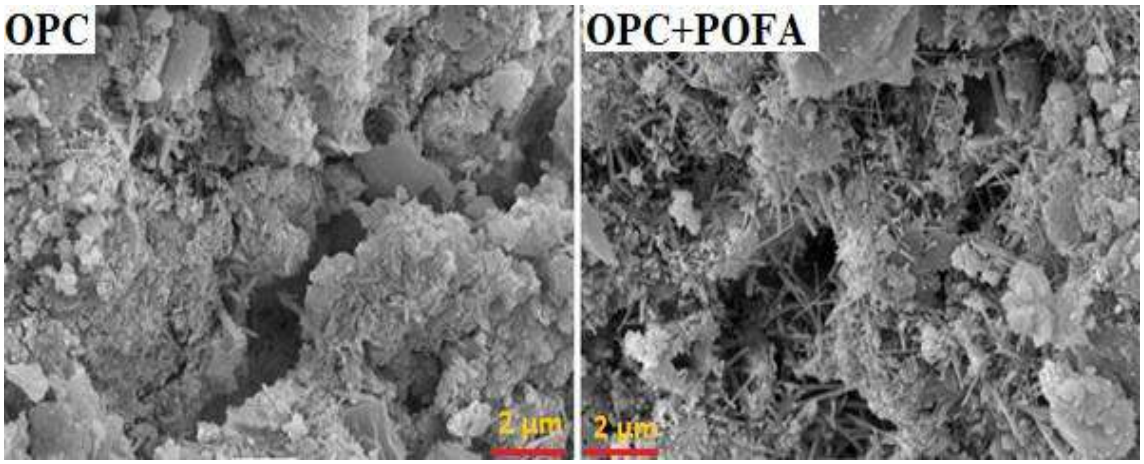

Figure 11. SEM images of OPC and POFA concrete mixes cured in water.

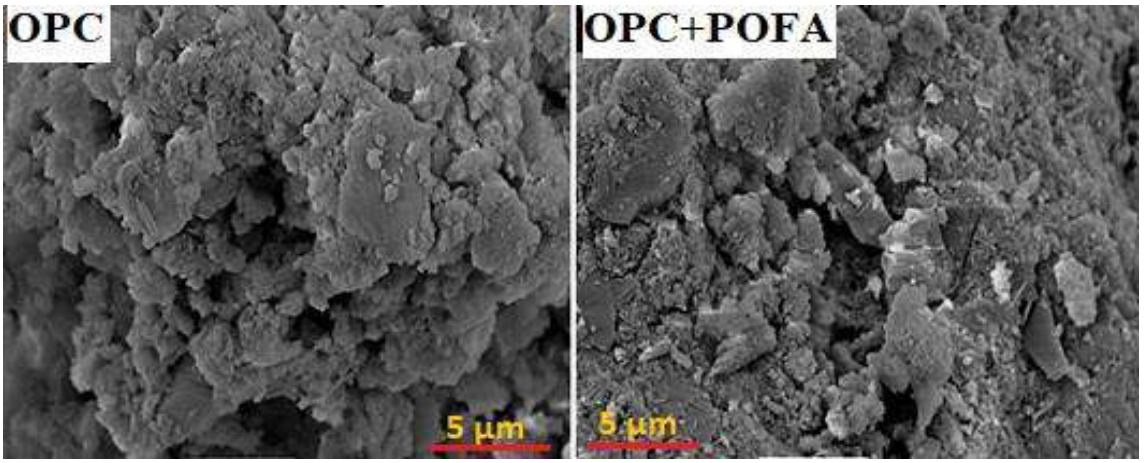

Figure 12. SEM images of OPC and POFA concrete mixes immersed in 5% NaCl solution.

Figure 12 also demonstrates alterations in the cellular structure of samples immersed in chloride solution. The sphere-shaped voids in the OPC mixtures gradually fill up with additional precipitated particles as the exposure time goes on. When POFA-containing mixes were immersed in chloride solution, however, the extra C-S-H crystals formed due to POFA's pozzolanic activity were less harmed by the chloride assault. The microstructure of the OPC mix is more variable than that of the POFA mix, implying that the concrete's durability is compromised. As a result, the presence of POFA densified the matrix, resulting in a decreased volume of voids and micro-cracks and improved concrete durability.

XRD analysis was also performed on the concrete samples after 90 days of curing and exposure to chloride solution to examine the variation in the mineralogy of the concrete samples cured in water and subjected to chloride solution. The main hydration products for concrete samples cured in water, as shown in Figure 13, are portlandite (P), gypsum (G), and quartz (Q) for both OPC and POFA specimens, but the calcium silicate hydrate (C-S-H) crystals have higher intensity in the POFA mix. When OPC was replaced with POFA, the peak intensities of Portlandite were significantly lowered, as demonstrated by the diffractogram peaks. This is due to an excess of reactive silica in the POFA mix, which combines with $Ca(OH)_2$ to generate an extra C-S-H gel during the hydration phase. When the cement was replaced with POFA, the peak intensities of the specimen were lowered, as seen in Figure 13. In the POFA mix, CH can chemically react with active SiO_2 in significant amounts to form extra C-S-H gels, which improve concrete strength and durability. As seen in XRD figures illustrating POFA, the sample is dominated by strong C-S-H peaks at 2-θ of 28.8°. Because it creates an unbroken compound that bonds the cement particles into a cohesive mass, the C-S-H is responsible for most of the engineering qualities of concrete. Furthermore, gypsum ($CaSO_4 \cdot 2H_2O$) is detected in trace levels in POFA and OPC samples. The presence of gypsum in cement retards the C_3A's reaction to flash setting. The gypsum breaks down and combines with the C_3A to generate ettringite as water is introduced to the combination ($3CaO \cdot Al_2O_3 \cdot 3CaSO_4 \cdot 32H_2O$). Ettringite is formed from very fine-grained crystals that form a coating on the surface of C_3A particles [45].

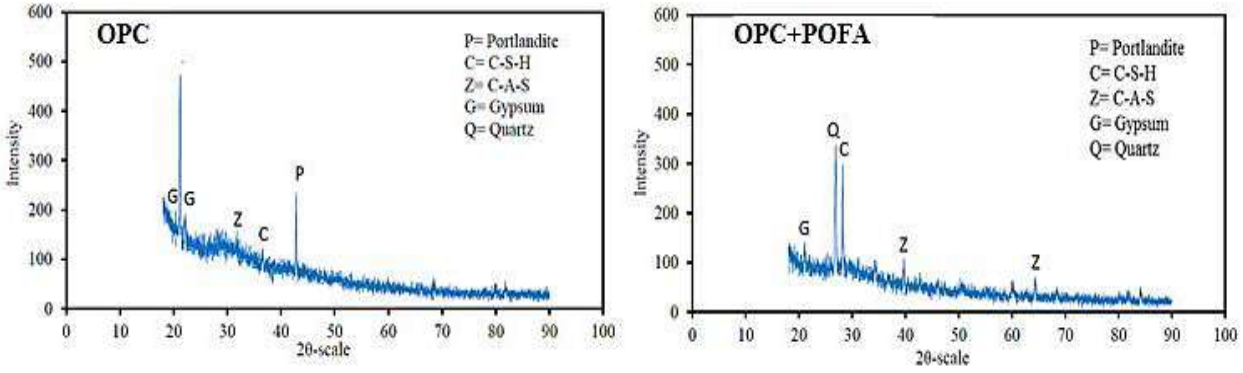

Figure 13. XRD analysis of OPC and POFA concrete mixes cured in water.

In addition, XRD analysis was performed on the concrete samples immersed in chloride solution, and the findings are shown in Figure 14. The results of the XRD examination demonstrated that chloride ions penetrated concrete specimens and induced considerable morphological changes in concrete mixes, mainly the OPC mixture. The formation of Friedel's salt showed the development of new components in the matrix due to chloride attack, and $Ca(OH)_2$ is still present in the matrix after chloride exposure. The XRD data show that the OPC mix has a higher intensity of Friedel's salt than the POFA mix, which could be due to the presence of cavities that allow chloride ions to enter the OPC specimen. The addition of C-S-H gels to POFA mixtures resulted in a solid matrix with improved durability and a lower chloride penetration rate [46,47]. According to the XRD analysis, Friedel's salt is found in the POFA sample, although in a lower quantity than in the OPC specimen.

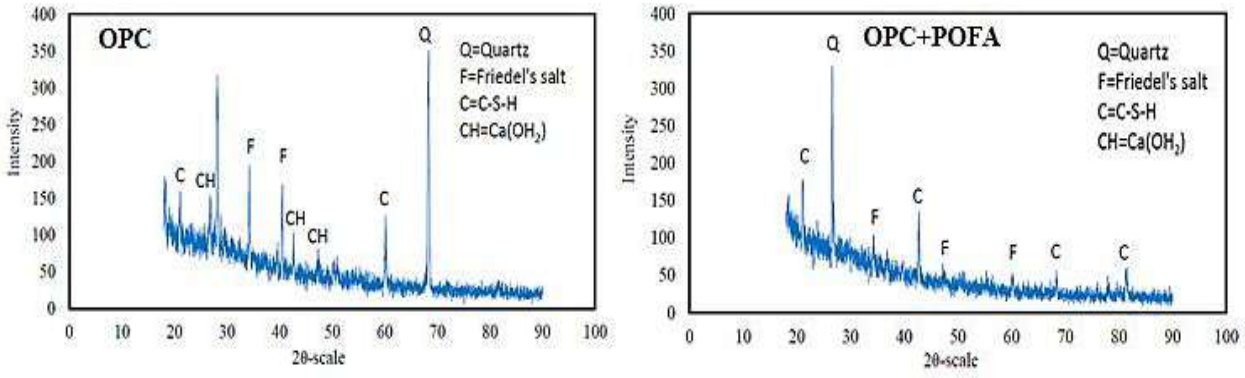

Figure 14. XRD analysis of OPC and POFA mixes immersed in 5% NaCl solution.

4. Conclusions

The impact of waste metalized film food packaging (MFP) fibers at different volume fractions and palm oil fuel ash as a partial cement substitute on the strength and durability properties of concrete composites are investigated in this study. The experimental research yielded the following findings:

- The inclusion of MFP fibers in concrete mixes reduced the compressive strength slightly. The addition of mineral admixtures in concrete, on the other hand, increases compressive strength during extended curing times. POFA densifies concrete microstructure and improves the concrete's properties at more extended curing periods.
- MFP fibers improve the concrete's tensile strength while significantly increasing its ductility. In general, the larger the fiber volume percentage in the concrete mixes, the more significant the increase in tensile strength. The bond between fibers and the cement matrix inhibits micro-cracks from spreading and enhances the concrete's post-cracking behavior.
- MFP fibers up to 0.5% in the OPC mixes reduced the carbonation depth by about 16% after 180-day exposure to CO_2. Due to POFA's slower pozzolanic reactivity, the inclusion of POFA in the concrete mixtures caused a greater carbonation depth than OPC mixes.
- The drying shrinkage of OPC and POFA reinforced concrete mixtures was considerably influenced by MFP fibers in all volume fractions. For a concrete composite that contained 0.75% MFP fibers and 20% POFA after 180 days of testing, drying shrinkage was decreased by about 30%.
- The addition of POFA and MFP fibers to concrete mixes substantially impacts their durability. The mixture of MFP fiber and POFA simultaneously produces the best durability of all the concretes studied. Compared to plain OPC concrete, the chloride penetration of the mix with 20% POFA and 0.75% MFP fibers was decreased by approximately 10% after 90 days. Furthermore, associated with the control mix, the electrical resistance of the same combination rose by roughly 80% at the same age.
- The microstructural investigation of the OPC matrix showed voids dispersed throughout the paste structure. POFA paste morphology revealed dense, amorphous, and impermeable compounds, with unreacted ash particles serving as filler to produce a dense matrix. The densification of the matrix with more hydration products was related to the higher durability efficiency of concrete composites.
- With the addition of MFP fibers, the concrete specimen's chloride penetration is reduced while its electrical resistance is raised. The reinforced specimens may be classed as "high" resistance against chloride penetration and "low" rebar corrosion rate based on the 90-day chloride penetration and electrical resistivity tests.

Author Contributions: All authors contributed to the paper evenly. Conceptualization, H.M., S.P.N. and R.A.; methodology, A.A.K.E., A.M.M. and R.A.; software S.P.N. and R.A.; validation, H.M., A.A.K.E. and R.A.; formal analysis, H.M., A.M.M. and R.A.; investigation, H.A., A.M.M. and R.A.; resources, H.M., A.M.M. and R.A.; data curation, H.M. and R.A.; writing—original draft preparation, H.M., H.A. and R.A.; writing—review and editing, H.M., A.A.K.E. and R.A.; visualization, H.M. and S.P.N.; supervision, H.A. and A.A.K.E.; project administration, R.A. and S.P.N.; funding acquisition, H.M. and R.A. All authors have read and agreed to the published version of the manuscript.

Funding: The authors extend their appreciation to the Deputyship for Research & Innovation, Ministry of Education in Saudi Arabia, for funding this research work through the project number IF-PSAU-2021/01/18918.

Institutional Review Board Statement: Not applicable.

Informed Consent Statement: Not applicable.

Data Availability Statement: The data presented in this study are available on request from the corresponding author.

Acknowledgments: The authors would like to acknowledge the technical support received from Prince Sattam Bin Abdulaziz University (Saudi Arabia) and Universiti Teknologi Malaysia.

Conflicts of Interest: The authors declare no conflict of interest.

References

1. Sun, C.; Chen, Q.; Xiao, J.; Liu, W. Utilization of waste concrete recycling materials in self-compacting concrete. *Resour. Conserv. Recycl.* **2020**, *161*, 104930. [CrossRef]
2. Choudhary, J.; Kumar, B.; Gupta, A. Feasible utilization of waste limestone sludge as filler in bituminous concrete. *Constr. Build. Mater.* **2020**, *239*, 117781. [CrossRef]
3. Mohammadhosseini, H.; Yatim, J.M.; Sam, A.R.M.; Awal, A.A. Durability performance of green concrete composites containing waste carpet fibers and palm oil fuel ash. *J. Clean. Prod.* **2017**, *144*, 448–458. [CrossRef]
4. Siddique, R.; Singh, G. Utilization of waste foundry sand (WFS) in concrete manufacturing. *Resour. Conserv. Recycl.* **2011**, *55*, 885–892. [CrossRef]
5. Alaskar, A.; Alqarni, A.S.; Alfalah, G.; El-Sayed, A.K.; Mohammadhosseini, H.; Alyousef, R. Performance evaluation of reinforced concrete beams with corroded web reinforcement: Experimental and theoretical study. *J. Build. Eng.* **2021**, *35*, 102038. [CrossRef]
6. Mohammadhosseini, H.; Alyousef, R.; Poi Ngian, S.; Tahir, M.M. Performance evaluation of sustainable concrete comprising waste polypropylene food tray fibers and palm oil fuel ash exposed to sulfate and acid attacks. *Crystals* **2021**, *11*, 966. [CrossRef]
7. Gu, L.; Ozbakkaloglu, T. Use of recycled plastics in concrete: A critical review. *Waste Manag.* **2016**, *51*, 19–42. [CrossRef]
8. Sharma, R.; Bansal, P.P. Use of different forms of waste plastic in concrete—A review. *J. Clean. Prod.* **2016**, *112*, 473–482. [CrossRef]
9. Saikia, N.; de Brito, J. Use of plastic waste as aggregate in cement mortar and concrete preparation: A review. *Constr. Build. Mater.* **2012**, *34*, 385–401. [CrossRef]
10. Albano, C.; Camacho, N.; Hernández, M.; Matheus, A.; Gutiérrez, A. Influence of content and particle size of waste pet bottles on concrete behavior at different w/c ratios. *Waste Manag.* **2009**, *29*, 2707–2716. [CrossRef]
11. Eriksen, M.; Christiansen, J.; Daugaard, A.E.; Astrup, T. Closing the loop for PET, PE and PP waste from households: Influence of material properties and product design for plastic recycling. *Waste Manag.* **2019**, *96*, 75–85. [CrossRef] [PubMed]
12. Faraca, G.; Astrup, T. Plastic waste from recycling centres: Characterisation and evaluation of plastic recyclability. *Waste Manag.* **2019**, *95*, 388–398. [CrossRef] [PubMed]
13. Hahladakis, J.N.; Iacovidou, E. An overview of the challenges and trade-offs in closing the loop of post-consumer plastic waste (PCPW): Focus on recycling. *J. Hazard. Mater.* **2019**, *380*, 120887. [CrossRef]
14. Eriksen, M.; Astrup, T. Characterisation of source-separated, rigid plastic waste and evaluation of recycling initiatives: Effects of product design and source-separation system. *Waste Manag.* **2019**, *87*, 161–172. [CrossRef] [PubMed]
15. Mohammadhosseini, H.; Alyousef, R.; Lim, N.H.A.S.; Tahir, M.M.; Alabduljabbar, H.; Mohamed, A.M.; Samadi, M. Waste metalized film food packaging as low cost and ecofriendly fibrous materials in the production of sustainable and green concrete composites. *J. Clean. Prod.* **2020**, *258*, 120726. [CrossRef]
16. Mahmood, R.A.; Kockal, N.U. Cementitious materials incorporating waste plastics: A review. *SN Appl. Sci.* **2020**, *2*, 1–13. [CrossRef]
17. Buller, A.S.; Abro, F.U.R.; Lee, K.-M.; Jang, S.Y. Mechanical Recovery of Cracked Fiber-Reinforced Mortar Incorporating Crystalline Admixture, Expansive Agent, and Geomaterial. *Adv. Mater. Sci. Eng.* **2019**, *2019*, 3420349. [CrossRef]
18. Liu, F.; Zhang, T.; Luo, T.; Zhou, M.; Ma, W.; Zhang, K. The effects of Nano-SiO_2 and Nano-TiO_2 addition on the durability and deterioration of concrete subject to freezing and thawing cycles. *Materials* **2019**, *12*, 3608. [CrossRef]
19. Yi, Y.; Zhu, D.; Guo, S.; Zhang, Z.; Shi, C. A review on the deterioration and approaches to enhance the durability of concrete in the marine environment. *Cem. Concr. Compos.* **2020**, *113*, 103695. [CrossRef]
20. Paul, S.C.; Van Zijl, G.P.; Šavija, B. Effect of Fibers on Durability of Concrete: A Practical Review. *Materials* **2020**, *13*, 4562. [CrossRef]

21. Abro, F.U.R.; Buller, A.S.; Lee, K.-M.; Jang, S.Y. Using the Steady-State Chloride Migration Test to Evaluate the Self-Healing Capacity of Cracked Mortars Containing Crystalline, Expansive, and Swelling Admixtures. *Materials* **2019**, *12*, 1865. [CrossRef] [PubMed]
22. Buller, A.S.; Abro, F.-U.-R.; Ali, T.; Jakhrani, S.H.; Ul-Abdin, Z. Stimulated autogenous-healing capacity of fiber-reinforced mortar incorporating healing agents for recovery against fracture and mechanical properties. *Mater. Sci.* **2021**, *39*, 33–48. [CrossRef]
23. Alrshoudi, F.; Mohammadhosseini, H.; Md. Tahir, M.; Alyousef, R.; Alghamdi, H.; Alharbi, Y.R.; Alsaif, A. Sustainable use of waste polypropylene fibers and palm oil fuel ash in the production of novel prepacked aggregate fiber-reinforced concrete. *Sustainability* **2020**, *12*, 4871. [CrossRef]
24. Alnahhal, M.F.; Alengaram, U.J.; Jumaat, M.Z.; Alsubari, B.; Alqedra, M.A.; Mo, K.H. Effect of aggressive chemicals on durability and microstructure properties of concrete containing crushed new concrete aggregate and non-traditional supplementary cementitious materials. *Constr. Build. Mater.* **2018**, *163*, 482–495. [CrossRef]
25. Wang, W.; Shen, A.; Lyu, Z.; He, Z.; Nguyen, K.T. Fresh and rheological characteristics of fiber reinforced concrete—A review. *Constr. Build. Mater.* **2021**, *296*, 123734. [CrossRef]
26. Mujedu, K.A.; Ab-Kadir, M.A.; Ismail, M. A review on self-compacting concrete incorporating palm oil fuel ash as a cement replacement. *Constr. Build. Mater.* **2020**, *258*, 119541. [CrossRef]
27. Mohammadhosseini, H.; Alrshoudi, F.; Tahir, M.M.; Alyousef, R.; Alghamdi, H.; Alharbi, Y.R.; Alsaif, A. Durability and thermal properties of prepacked aggregate concrete reinforced with waste polypropylene fibers. *J. Build. Eng.* **2020**, *32*, 101723. [CrossRef]
28. Turk, K.; Bassurucu, M.; Bitkin, R.E. Workability, strength and flexural toughness properties of hybrid steel fiber reinforced SCC with high-volume fiber. *Constr. Build. Mater.* **2021**, *266*, 120944. [CrossRef]
29. Zhang, P.; Li, Q. Fracture properties of polypropylene fiber reinforced concrete containing fly ash and silica fume. *Res. J. Appl. Sci. Eng. Technol.* **2013**, *5*, 665–670. [CrossRef]
30. Li, Y.; Su, Y.; Tan, K.H.; Zheng, X.; Sheng, J. Pore structure and splitting tensile strength of hybrid Basalt–Polypropylene fiber reinforced concrete subjected to carbonation. *Constr. Build. Mater.* **2021**, *297*, 123779. [CrossRef]
31. Bao, H.; Yu, M.; Chi, Y.; Liu, Y.; Ye, J. Performance evaluation of steel-polypropylene hybrid fiber reinforced concrete under supercritical carbonation. *J. Build. Eng.* **2021**, *43*, 103159. [CrossRef]
32. Almeida, A.E.F.S.; Tonoli, G.H.D.; Santos, S.F.; Savastano, H., Jr. Improved durability of vegetable fiber reinforced cement composite subject to accelerated carbonation at early age. *Cem. Concr. Compos.* **2013**, *42*, 49–58. [CrossRef]
33. Tang, W.L.; Lee, H.-S.; Vimonsatit, V.; Htut, T.; Singh, J.K.; Hassan, W.N.F.W.; Ismail, M.A.; Seikh, A.H.; Alharthi, N. Optimization of Micro and Nano Palm Oil Fuel Ash to Determine the Carbonation Resistance of the Concrete in Accelerated Condition. *Materials* **2019**, *12*, 130. [CrossRef] [PubMed]
34. Mohammadhosseini, H.; Alrshoudi, F.; Tahir, M.M.; Alyousef, R.; Alghamdi, H.; Alharbi, Y.R.; Alsaif, A. Performance evaluation of novel prepacked aggregate concrete reinforced with waste polypropylene fibers at elevated temperatures. *Constr. Build. Mater.* **2020**, *259*, 120418. [CrossRef]
35. Karahan, O.; Atis, C. The durability properties of polypropylene fiber reinforced fly ash concrete. *Mater. Des.* **2011**, *32*, 1044–1049. [CrossRef]
36. Teng, S.; Afroughsabet, V.; Ostertag, C.P. Flexural behavior and durability properties of high performance hybrid-fiber-reinforced concrete. *Constr. Build. Mater.* **2018**, *182*, 504–515. [CrossRef]
37. Wang, L.; Aslani, F. Electrical resistivity and piezoresistivity of cement mortar containing ground granulated blast furnace slag. *Constr. Build. Mater.* **2020**, *263*, 120243. [CrossRef]
38. Neville, A.M.; Brooks, J.J. *Concrete Technology*, 2nd ed.; Longman Scientific & Technical: London, UK, 2010.
39. Lim, T.Y.D.; Teng, S.; Bahador, S.D.; Gjørv, O.E. Durability of Very-High-Strength Concrete with Supplementary Cementitious Materials for Marine Environments. *ACI Mater. J.* **2016**, *113*, 95–103. [CrossRef]
40. Zhang, M.; Li, H. Pore structure and chloride permeability of concrete containing nano-particles for pavement. *Constr. Build. Mater.* **2011**, *25*, 608–616. [CrossRef]
41. Abro, F.U.R.; Buller, A.S.; Ali, T.; Ul-Abdin, Z.; Ahmed, Z.; Memon, N.A.; Lashari, A.R. Autogenous Healing of Cracked Mortar Using Modified Steady-State Migration Test against Chloride Penetration. *Sustainability* **2021**, *13*, 9519. [CrossRef]
42. Afroughsabet, V.; Biolzi, L.; Monteiro, P.J. The effect of steel and polypropylene fibers on the chloride diffusivity and drying shrinkage of high-strength concrete. *Compos. Part B Eng.* **2018**, *139*, 84–96. [CrossRef]
43. Kroehong, W.; Damrongwiriyanupap, N.; Sinsiri, T.; Jaturapitakkul, C. The Effect of Palm Oil Fuel Ash as a Supplementary Cementitious Material on Chloride Penetration and Microstructure of Blended Cement Paste. *Arab. J. Sci. Eng.* **2016**, *41*, 4799–4808. [CrossRef]
44. Alnahhal, A.M.; Alengaram, U.J.; Yusoff, S.; Singh, R.; Radwan, M.K.; Deboucha, W. Synthesis of sustainable lightweight foamed concrete using palm oil fuel ash as a cement replacement material. *J. Build. Eng.* **2021**, *35*, 102047. [CrossRef]
45. Kroehong, W.; Sinsiri, T.; Jaturapitakkul, C.; Chindaprasirt, P. Effect of palm oil fuel ash fineness on the microstructure of blended cement paste. *Constr. Build. Mater.* **2011**, *25*, 4095–4104. [CrossRef]
46. Mohammadhosseini, H.; Alyousef, R.; Md. Tahir, M. Towards Sustainable Concrete Composites through Waste Valorisation of Plastic Food Trays as Low-Cost Fibrous Materials. *Sustainability* **2021**, *13*, 2073. [CrossRef]
47. Alrshoudi, F.; Mohammadhosseini, H.; Alyousef, R.; Tahir, M.M.; Alabduljabbar, H.; Mustafa Mohamed, A. The impact resistance and deformation performance of novel pre-packed aggregate concrete reinforced with waste polypropylene fibres. *Crystals* **2020**, *10*, 788. [CrossRef]